Computational design and experimental validation of oligonucleotide-sensing allosteric ribozymes

Robert Penchovsky & Ronald R Breaker

Allosteric RNAs operate as molecular switches that alter folding and function in response to ligand binding. A common type of natural allosteric RNAs is the riboswitch; designer RNAs with similar properties can be created by RNA engineering. We describe a computational approach for designing allosteric ribozymes triggered by binding oligonucleotides. Four universal types of RNA switches possessing AND, OR, YES and NOT Boolean logic functions were created in modular form, which allows ligand specificity to be changed without altering the catalytic core of the ribozyme. All computationally designed allosteric ribozymes were synthesized and experimentally tested *in vitro*. Engineered ribozymes exhibit $> 1,000$-fold activation, demonstrate precise ligand specificity and function in molecular circuits in which the self-cleavage product of one RNA triggers the action of a second. This engineering approach provides a rapid and inexpensive way to create allosteric RNAs for constructing complex molecular circuits, nucleic acid detection systems and gene control elements.

The detection of specific chemical and biological compounds can be achieved with structured RNAs that form selective binding pockets for their target ligands[1]. These ligand-binding domains, or aptamers[2,3], can be used independently[4–6] or can be joined with other functional RNA domains[7–9] to serve as molecular reporter systems that selectively bind targets and signal their presence to the user. For example, aptamers have been judiciously coupled to catalytic RNA domains to form allosteric ribozymes whose activities in many cases are modulated by several orders of magnitude upon ligand (or 'effector') binding[8].

The potential utility of allosteric ribozymes has been demonstrated by the construction of prototype RNA sensor arrays that have been used to detect specific proteins, small molecules and metal ions that are present even in complex biological mixtures[10,11]. Furthermore, it has recently been discovered that numerous natural RNA switches, or riboswitches, exist in many bacteria[12–15] and in some higher organisms[16,17], where they serve as metabolite-sensing gene control elements[18–20]. The fact that modern organisms rely on riboswitches supports the hypothesis that nucleic acids provide a robust medium for the construction of such functional macromolecules. Indeed, novel allosteric RNAs might be engineered for a broad range of practical applications[1] in areas such as gene therapy[21,22], designer gene control systems[23–27], biosensors[10,11,28–30] and molecular computation[31,32].

The fusion of aptamers with ribozymes to create RNA switches most commonly has been achieved by modular rational design[33,34], or by blending modular rational design with *in vitro* evolution techniques[35–37]. Modular rational design approaches are most effective for designing oligonucleotide-responsive ribozymes[38–41] or deoxyribozymes[42,43], largely because the rules that govern molecular recognition and structural characteristics of Watson-Crick base-paired interactions

are well understood. However, it remains problematic to design allosteric nucleic acids that exhibit robust activation, that are triggered without introducing denaturation and reannealing steps and that process to near completion.

In this study, we describe a computational strategy for designing new allosteric ribozyme constructs that exhibit robust allosteric activation upon the addition of specific oligonucleotides. A partition function algorithm[44] was used to design RNAs that are predicted to form a dominant secondary structure in the absence of an oligonucleotide effector. This folded pattern is predicted to be distinct from the secondary structure that dominates in the presence of a matched oligonucleotide effector. The algorithm computes the entire ensemble of possible secondary structures as a function of temperature[45], which allows the user to choose to build only those constructs that are predicted to exhibit the desired molecular switch characteristics.

This automated design method can be used to generate a large number of allosteric ribozymes with predefined properties within hours by assessing millions of different sequences on a personal computer. We demonstrate the utility of this method by designing and testing four universal types of molecular switches possessing AND, OR, NOT and YES Boolean logic functions. Each ribozyme construct has a modular architecture, which allows an oligonucleotide binding site (from 16 to 22 nt in length) to be computationally altered, thus maintaining specific and uniform allosteric function.

RESULTS
Architecture and design of allosteric hammerhead ribozymes
As is observed with allosteric proteins, RNAs with allosteric function undergo alternative folding of their polymeric structure upon effector binding, which modulates of function at a site that is distal from

Department of Molecular, Cellular and Developmental Biology, Yale University, PO Box 208103, New Haven, Connecticut 06520-8103, USA. Correspondence should be addressed to R.R.B. (ronald.breaker@yale.edu).
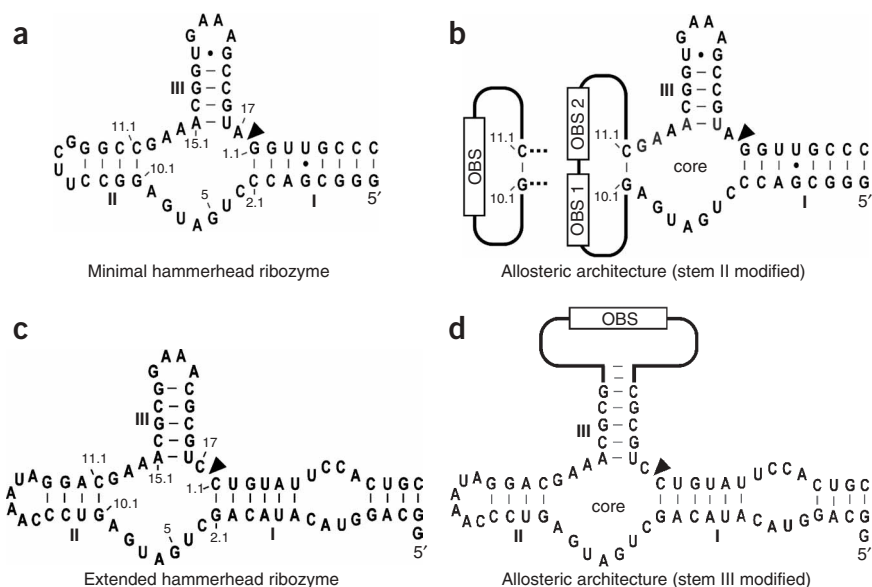
Figure 1 Design architectures for the construction of oligonucleotide-responsive hammerhead ribozymes. (**a**) Parental hammerhead ribozyme sequence used previously[33–36] and in the current study to create ligand-responsive ribozyme switches. Numbering systems for the hammerhead is as described elsewhere[52], where stems I through III represent base-paired structures that are essential for ribozyme function. The arrowhead identifies the site of ribozyme self-cleavage. (**b**) Integration of one (left) or two (right) oligonucleotide binding sites (OBS) into stem II of the parent hammerhead depicted in **a**. (**c**) Extended hammerhead ribozyme that exhibits faster RNA cleavage rates with low Mg^{2+} concentrations[53]. (**d**) Integration of an OBS in stem I of the extended ribozyme to create RNA switches with NOT function.

where the effector has bound. In the case of RNA, stable secondary structures can fold on a time scale of microseconds, and these core elements typically control the subsequent formation of tertiary contacts[46–48]. The energies involved in secondary structure formation typically are much greater than those of tertiary contacts[49]. Thus, a substantial amount of the folding energy that establishes RNA conformations can be modeled at the secondary structure level[50]. However, alternative stable conformations could form at various stages of the folding process and trap the molecule into an inactive conformation. Thus, a broader landscape of folding potential should be taken into account to minimize the probability of encountering such misfolded conformers.

The precise secondary structure required for the hammerhead ribozyme to promote RNA transesterification is well known (**Fig. 1a**)[51,52]. Variations in sequence composition that preclude formation of this essential secondary structure most likely will result in reduced activity, or no activity at all. Allosteric ribozymes can exploit this character of RNA structure by harnessing binding energy involved in effector-RNA complex formation to shift folding patterns or pathways to favor either active or inactive states. If these states are separated by a large energy barrier (e.g., strong base-pairing interactions must be disrupted to exchange states), then the ribozyme cannot transition easily between the two states without more proactive denaturation and reannealing. In contrast, if the energy barrier between the two states is small, then the ribozyme might exhibit a poor dynamic range for modulation by the effector. It is these aspects of allosteric ribozyme design that have been most difficult to anticipate and control during the design process.

The architecture of most ribozyme constructs chosen for this study exploit the sequence versatility of nucleotides residing in stem II of the hammerhead ribozyme (**Fig. 1b**). This same region has been used extensively as the location for grafting aptamers when creating numerous other allosteric ribozyme constructs[10,33–36]. An extended hammerhead construct (**Fig. 1c**) was used to introduce allosteric binding sites into stem III (**Fig. 1d**). A two-step computational procedure was applied to design allosteric hammerhead ribozymes that modulate their cleavage activity only in the presence of predefined oligonucleotides. In the first step, a large number of random sequences ($\geq 10^7$) residing within the effector binding

site(s) were examined computationally using a random search algorithm based on the partition function for formation of dominant secondary structures[44] in the presence and absence of effector molecules with different lengths. Nucleotide sequences residing within an oligonucleotide binding site (OBS) must satisfy two criteria for a given construct to be chosen for testing. First, OBS nucleotides must be predicted to participate in forming stable but inactive secondary structure (OFF state) in the absence of an effector oligonucleotide. Second, OBS nucleotides must stably pair with the effector DNA and liberate adjoining nucleotides that are predicted to form a stable stem II structure that allows activation of the ribozyme domain (ON state).

Design and characterization of ribozymes with YES function

Using the approach described above, we generated a series of five RNA constructs that were predicted to function as RNA switches with molecular YES logic. Molecules with attributes of YES logic function must remain inactive unless receiving a single molecular impulse that triggers activity. One of these constructs, termed YES-1, is predicted to form the desired OFF- and ON-state structures in the absence and presence, respectively, of a 22-nt effector DNA (DNA-1; **Fig. 2a**). In its inactive conformation, the nucleotides within the OBS are proposed to form a stem IV structure. Stem IV involves extensive base-pairing interactions with portions of the hammerhead core and with most nucleotides that would otherwise form the stem II structure required for ribozyme activation. In the presence of DNA-1, a major portion of the nucleotides in stem IV would become sequestered by intermolecular base pairing, and nucleotides that can participate in stem II formation are liberated.

The results of the computational assessment of the structure-forming potential of this construct are visually represented by dot matrix plots (**Fig. 2a**, right). It is apparent from these plots that the probability of forming stem IV or several base-pairing alternatives is high, whereas there is no indication that stem II has any reasonable chance of forming. In contrast, repeating the computation in the presence of the DNA effector drastically reduces the probability that stem IV can form and thus increases the probability that stem II will be formed. It is notable that the probabilities for forming hammerhead stems I and III remain largely unaffected by the

Figure 2 Design and characterization of an oligonucleotide-specific RNA switch possessing YES logic function. (**a**) Secondary structure models for the most stable conformers as computed using the partition function algorithm in the absence (OFF) or presence (ON) of a 22-nucleotide DNA effector. The effector-binding site (light blue) is joined to nucleotides 10.1 and 11.1 of the hammerhead core via eight- and six-nucleotide linkers. In the ON state, most of these linker nucleotides are predicted to form an extended stem II structure (red). To the right of each model is a dot matrix plot wherein larger points reflect greater probability of base pairing. Encircled points reflect the main differences in predicted structures between the OFF (stem IV) and ON (stem II) states. Nucleotides 1 through 79 are numbered from 5′ to 3′ across the top and right of the plots. Schematic representations of the logic states of the constructs are shown in this and subsequent figures. (**b**) Selective activation of ribozyme self-cleavage by an effector DNA complementary to the OBS. Radiolabeled ribozymes (5′ ^{32}P, Pre) undergo self-cleavage only with the perfectly matched DNA effector (0 mismatches) and the resulting radiolabeled cleavage fragment (Clv) is separated from the precursor by denaturing 10% PAGE. Products were visualized and cleavage yields were quantified by PhosphorImager. (**c**) Kinetics of ribozyme (1 μM) self-cleavage in the presence (+) of perfectly matched 22-nt effector DNA (3 μM) and in the absence (–) of effector DNA. Gel image is as described in **b**. Plot using data derived from the gel depicts the natural logarithm of the fraction of RNA remaining uncleaved versus time.
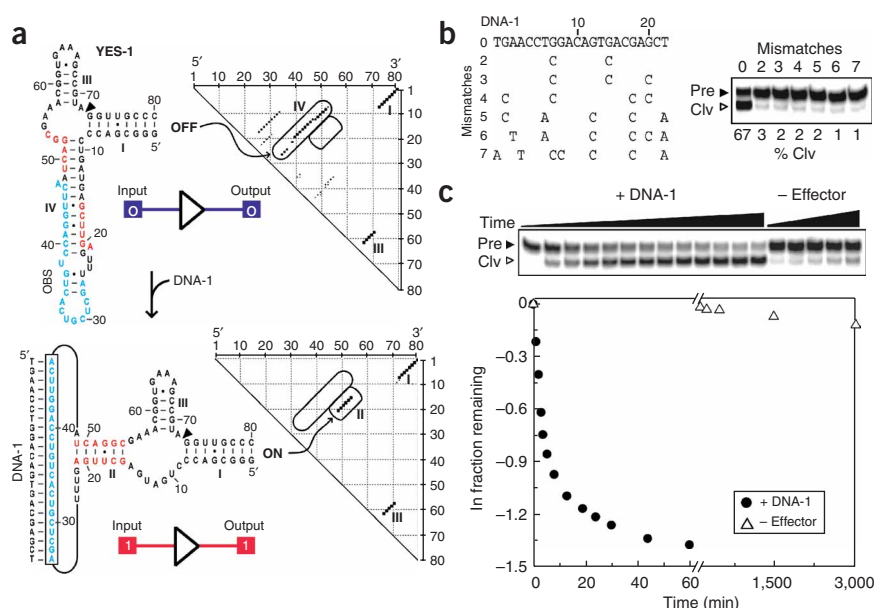

presence or absence of the effector DNA. In a subsequent stage of the design procedure, the secondary structure adopted for the YES-1 ribozyme was used as a basis to compute the folding properties of additional allosteric ribozyme candidates that are likely to have very similar RNA energy folding landscapes but that carry different OBS sequences that respond to different effector DNAs.

Five sequences obtained from this computational design process, representing extreme cases in terms of the selection thermodynamics criteria used during computation, were arbitrarily chosen for synthesis and testing. Each RNA construct was prepared by transcription *in vitro* using radiolabeled nucleotides. The YES-1 RNA construct (**Fig. 2a**) is representative of ribozyme constructs that were computed to be thermodynamically less stable in their inactive states (free energy based on the partition function at 37 °C, $E_p = -35.6$ kcal mol^{-1}) and are predicted to have the potential to form several alternative secondary structures that all preclude formation of stem II.

The performance characteristics of the first RNA, YES-1, was tested by incubation of internally ^{32}P-labeled RNAs with a matched effector DNA of 22 nt, or with a series of mutant DNAs that carry two through seven mismatches relative to the matched effector DNA (**Fig. 2b**). Robust self-cleavage was observed only when the perfectly matched effector DNA was present, whereas as few as two mismatches caused complete loss of activation under these assay

conditions. From these data, we conclude that the thermodynamic stability of the OFF state for YES-1 is sufficiently greater than that of the ON state in the absence of effector DNA ($E_p = -29$ kcal mol^{-1}, difference = 6.6 kcal mol^{-1}) such that the vast majority of the RNA constructs reside in the inactive conformation during assay incubation.
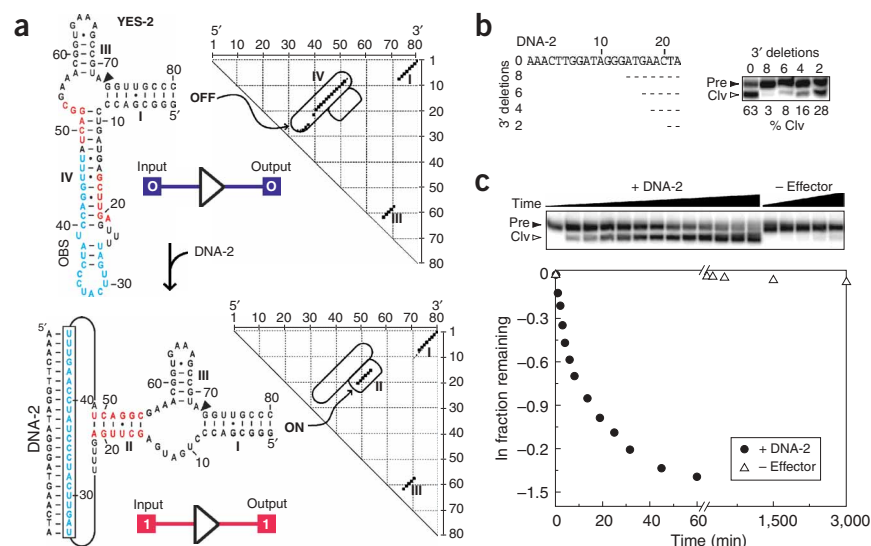
Figure 3 Design and characterization of YES-2, a variant of YES-1 that exhibits altered oligonucleotide specificity. (**a**) Secondary structure models for the most stable conformers in the absence (OFF) or presence (ON) of a 22-nucleotide DNA effector complementary to the changed OBS. (**b**) Selective activation of YES-2 self-cleavage by effector DNAs complementary to the OBS. (**c**) Kinetics of YES-2 self-cleavage in the presence of perfectly matched 22-nt effector DNA and in the absence of effector DNA. For additional details, see the legend to **Figure 2**.

To estimate the dynamic range for allosteric activation, or the total range of rate constant enhancement brought about by effector binding, we conducted a time course for ribozyme self-cleavage in the presence and absence of the matched effector DNA (**Fig. 2c**). In the presence of the effector, the apparent rate constant observed for ribozyme activity (apparent k_{obs}) is $\sim 1.1 \times 10^{-1}$ min^{-1}, whereas the apparent k_{obs} for the ribozyme in the absence of effector DNA is $\sim 1.6 \times 10^{-5}$ min^{-1}. These results indicate that the allosteric dynamic range is nearly 7,000-fold, and the maximum rate constant is within tenfold of the typical maximum activity for the unmodified hammerhead ribozyme core (~ 1 min^{-1}) measured under similar conditions[33]. Furthermore, the stability of the OFF-state structure is not so extreme or so rapidly adopted that activation by the effector DNA is precluded when reaction buffer (**Fig. 2b**) and DNA are introduced simultaneously to the YES-1 ribozyme.

Approximately 21% of the YES-1 RNAs that are incubated for 60 min in the presence of effector DNA remain uncleaved, suggesting that perhaps defects in RNA integrity or alternately folded RNAs preclude proper function of all RNAs in the reaction. To confirm the apparent k_{obs} value reported for ribozyme-effector complexes, we conducted additional experiments using 6 μM of effector DNA. The curve obtained was completely overlapping with that obtained when 3 μM effector DNA was used (data not shown), indicating that the ribozymes were saturated with effector DNA.

Similarly, the performance characteristics of a second ribozyme, YES-2 (**Fig. 3**), were established. YES-2 was selected for testing because it is predicted to be more stable in its OFF state ($E_p = -39$ kcal mol^{-1}) than YES-1, although it has a greater difference between the OFF- and ON-states ($E_p = -29$ kcal mol^{-1}, difference = 10 kcal mol^{-1}). This increase in predicted stability for stem IV yields dot matrix plots that suggest only one OFF-state structure that has a high probability of forming (**Fig. 3a**), whereas the addition of the effector DNA (DNA-2) that matches the new OBS sequences yields a predicted structure for the ribozyme domain that is identical to that for YES-1.

For this series of experiments, we tested the specificity of effector-mediated activation by using DNAs that differ from the matched YES-1 effector DNA by truncation **Fig. 3b**). Although the shortest effector DNA exhibits almost no activation of the YES-2 ribozyme, longer DNAs induce progressively greater yields, with the full-length effector DNA promoting ribozyme cleavage with a yield that is similar to that generated by the YES-1 ribozyme under identical reaction conditions (**Fig. 2b**).

The apparent k_{obs} values exhibited by the YES-2 ribozyme in the presence and absence of its matched 22-nt effector DNA also were similar to those observed for YES-1 (**Fig. 3c**), despite the differences in thermodynamic stability and predicted structural heterogeneity between the two constructs. Specifically, the dynamic range for YES-2 is $\sim 8,000$ with apparent k_{obs} values of 1.2×10^{-5} min^{-1} and 0.1 min^{-1} in the absence and presence of DNA-2, respectively.

Approximately 25% of YES-2 RNAs remain uncleaved after a 60-min incubation with the full-length DNA-2 (**Fig. 3c**), again suggesting that chemical integrity and/or folding uniformity are not absolute.

Similar molecular switch functions were obtained for the remaining three related constructs (YES-3, YES-4 and YES-5; **Supplementary Figs. 1–3** online), demonstrating that new RNA switches that respond to distinct DNA effectors can be designed routinely. Furthermore, these constructs function as 'rapid switches,' wherein the addition of the matched effector DNA induces activity in an RNA that had been folded into its inactive structure (**Supplementary Figs. 1–3** online). Alternatively, a construct that was intentionally designed to form an exceptionally stable OFF state structure (YES-6) remains inactive as expected, even upon the introduction of its matched DNA effector (**Supplementary Fig. 4** online). These results indicate that the computational method used to design multistate oligonucleotide-responsive ribozyme structures is robust and has a high probability of accurately predicting allosteric function. With the 22-nt long allosteric binding sites, there are 1.76×10^{13} possible sequence combinations, thus providing an enormous diversity of possible effector specificities. We predict that at least 5% of all possible combinations, or nearly a trillion different sequence combinations of 22-nt DNAs, will meet the rigorous criteria used in this study when designing candidate YES gates.

Design and characterization of a ribozyme with NOT function

An extended natural hammerhead ribozyme (**Fig. 1c**) from *Schistosoma mansoni* was used as the parent construct for the design of a ribozyme that is deactivated by allosteric interactions with oligonucleotides. This ribozyme exhibits faster RNA cleavage kinetics and requires lower concentrations of Mg^{2+} to trigger activity[53]. Allosteric constructs derived from parental ribozymes with these properties are more likely to function *in vivo* where divalent ion concentrations are low and where fast ribozymes might be needed.

Extended hammerhead ribozymes exhibit improved function because they form a tertiary structure between the loop sequences of stem II and a bulge within stem I[54–56]. Therefore, the OBS was relocated to stem III to design a construct that functions as a NOT gate (**Fig. 1d**) so these critical ribozyme tertiary-structure contacts would not be disrupted. The resulting design, termed NOT-1 (**Fig. 4a**) is predicted to form (**Supplementary Fig. 5** online) a single major ON state structure ($E_p = -30.55$ kcal mol^{-1}) in the absence of effector DNA-6 (23 nt), and is predicted to form a single major structure in its effector-bound OFF state that has an extended stem I and a disrupted stem III ($E_p = -25.46$ kcal mol^{-1}).

If the NOT-1 construct functions as predicted and self-cleaves in the absence of effector DNA, preparation of the RNA is expected to pose a
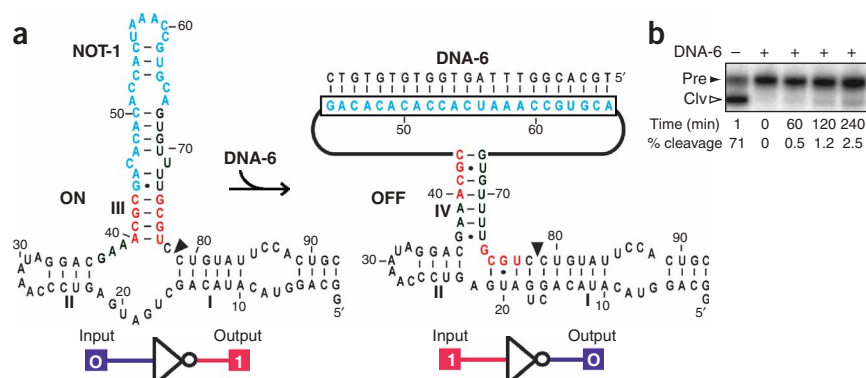
Figure 4 Design and characterization of NOT-1 based on an extended hammerhead ribozyme. (**a**) Secondary structure models for the most stable conformers predicted in the absence (ON) and presence (OFF) of a 23-nucleotide effector. Dot matrix plots for the construct are presented in **Supplementary Figure 5** online. (**b**) Deactivation of NOT-1 by a DNA complementary to the OBS.

Figure 5 Design and characterization of AND-1, an oligonucleotide-specific molecular switch that possesses AND logic function. (**a**) AND-1 is designed to form the active hammerhead structure and self-cleave only when presented simultaneously with its two corresponding effector DNAs (DNA-7 and DNA-8). The dot matrix plots for the ON state showing some character of the OFF states (stem IV) is depicted. Dot matrix plots for the three OFF states are presented in **Supplementary Figure 7** online. (**b**) Activation of AND-1 self-cleavage requires both full-length DNA-7 and DNA-8 effectors. Maximum incubation time is 60 min. (**c**) Kinetics of AND-1 self-cleavage under various combinations of effector DNAs. Details are as described in the legend to **Figure 2**.

problem because the ribozyme could self-cleave during transcription *in vitro*. To avoid this, we carried out transcription of NOT-1 DNA templates in the presence of 10 µM DNA-6 and 10 µM of the antisense oligonucleotide CTCATCAGC. The latter DNA is complementary to nucleotides 15 through 23 of the NOT-1 hammerhead core. Although the NOT-1 RNA exhibited only ~25% self-cleavage when produced by transcription under these conditions (data not shown), the RNA exhibited robust self-cleavage activity ($k_{obs} > 1$ min^{-1}) when incubated in the absence of DNA-6 (**Fig. 4b**). Similarly, addition of excess effector oligonucleotide to a NOT-1 ribozyme assay caused strong inhibition.

Design and characterization of a ribozyme with AND function

Molecules with attributes of AND logic function must remain inactive unless receiving two separate molecular impulses that trigger activity. Candidate RNA constructs possessing AND logic function triggered by 16-nt effector DNAs were designed using the same principles and computational procedures used to identify candidate YES RNA switches. However, additional steps were added to permit computation of four different structural states with high stability. As with the YES gate computations, one of the structural states must permit formation of the active hammerhead core, in this case, only when presented with two effector DNA sequences. The remaining three states should not permit ribozyme function even if either of the two effector DNAs are present independently. Our computational search efforts indicated that many thousands of ribozymes with the same AND gate properties can be generated.

We chose to test the function of one computationally designed AND gate candidate termed AND-1. The most probable secondary structure models for all four states of AND-1 and dot matrix plots for the predicted ON state are depicted in **Fig. 5a**. This RNA construct is predicted to have a thermodynamic stability in the absence of effector DNAs ($E_p = -46.97$ kcal mol^{-1}) that is ~15 kcal mol^{-1} more stable than the structure representing the active ribozyme state ($E_p = -31.9$ kcal mol^{-1}). The predicted stabilities of the RNA structures are intermediate when either effector DNA-7 ($E_p = -39.50$ kcal mol^{-1}) or effector DNA-8 ($E_p = -36.30$ kcal mol^{-1})
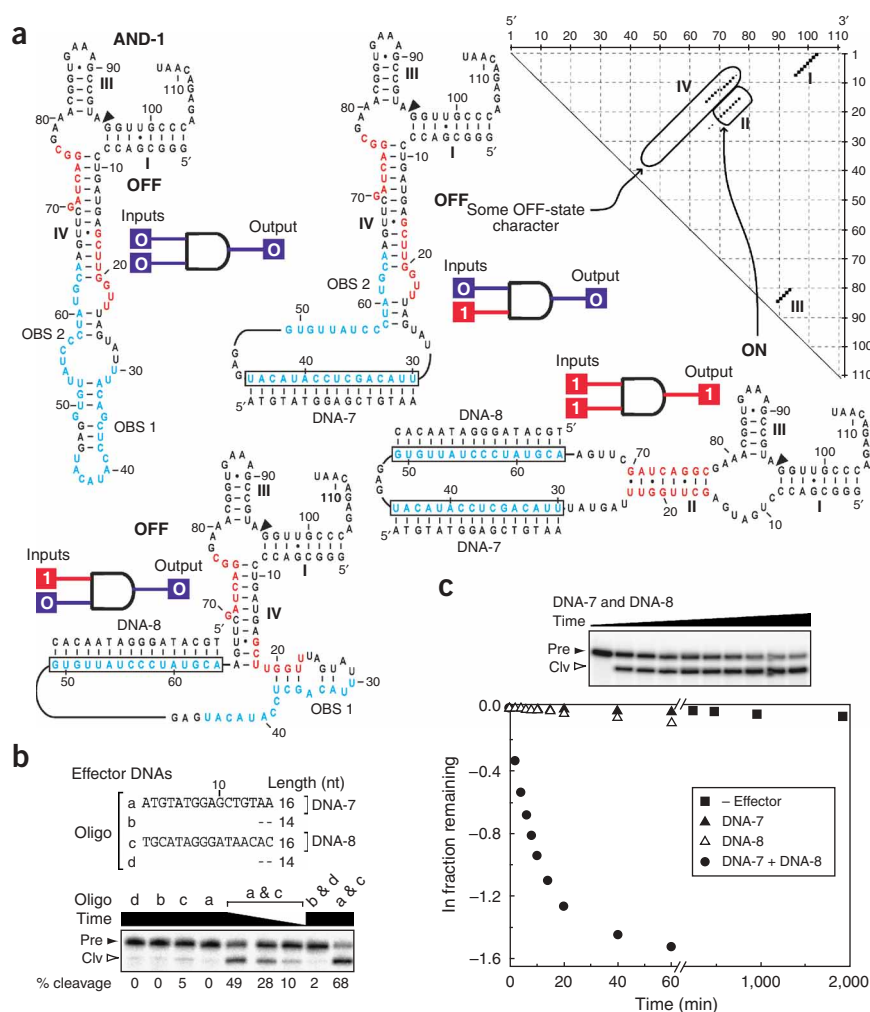
are bound independently. It is notable that, in the presence of both effectors, AND-1 is predicted to have approximately equal possibility for formation of stem II and a portion of stem IV, despite the docking of both effector DNAs (**Fig. 5a** and **Supplementary Fig. 6** online).

The general structural characteristics of AND-1 permit the ribozyme to remain largely inactive in the absence of effector DNAs, or in the presence of either DNA-7 or DNA-8 (**Fig. 5b**). However, the addition of both effector DNAs triggers robust ribozyme activity. The AND-1 ribozyme also is sensitive to the length of the effector DNAs. Although both 16-nt effector DNAs are needed to trigger AND-1 function, truncation of either DNA by deletion of two nucleotides at their 3′ terminus renders the system inactive, regardless of what combination of full-length and truncated DNAs are used (**Fig. 5b**).

To confirm our observations, we experimentally established rate constants for all four states with 1 µM AND-1 ribozyme incubated under standard reaction conditions (**Fig. 2b** legend) without and with 3 µM effector DNAs (**Fig. 5c**). Again, as computationally predicted, the AND-1 ribozyme exhibited very low self-cleavage activity in the absence of effector DNAs (apparent $k_{obs} = 2.4 \times 10^{-5}$ min^{-1}), and these poor apparent k_{obs} values persisted when either effector DNA-7 (1×10^{-4} min^{-1}) or effector DNA-8 (9×10^{-4} min^{-1}) were added independently. In contrast, the addition of both effectors induced an ~5,000-fold increase in the apparent k_{obs} value (0.11 min^{-1}) relative

to that exhibited by AND-1 in the absence of effector DNAs. This maximum apparent k_{obs} value increases to 0.5 min^{-1} when a single U-to-C change is made at nucleotide 18 (**Fig. 5a**), which strengthens base pairing in stem II (data not shown). Given the robust activity of the AND-1 ribozyme and its variant when activated, and given the extent to which these RNAs proceed towards complete processing, it is likely that the stem II structure dominates over the stem IV element (**Fig. 5a**) when presented with both effector DNAs, or at least the two stems are in rapid equilibrium.

Design and characterization of a ribozyme with OR function

The design of allosteric hammerhead ribozymes possessing OR logic function was conducted in a similar manner to that used to computationally identify AND gate candidates. Again four different states were computed, but in this case we sought to create three ON-state structures and only one OFF-state structure. Again, our computational search results indicate that many thousands of ribozymes with OR logic function can be designed. One candidate construct chosen for biochemical analysis, termed OR-1 (**Fig. 6a** and **Supplementary Fig. 7** online), carries only three nucleotide changes relative to the AND-1 RNA construct depicted in **Fig. 5a**. As with the other RNA logic gates described above, the most probable OFF state for OR-1 is thermodynamically more stable ($E_p = -46.5$ kcal mol^{-1}) than any of the ON-state structures that permit the formation of stem II ($E_p = -33.9$ kcal mol^{-1} when both effectors are bound).

The function of OR-1 also was tested for oligonucleotide-induced ribozyme activity. As predicted, OR-1 undergoes little self-cleavage in the absence of effector DNAs, but exhibits robust activity when presented with any combination of effectors DNA-9 and DNA-10, which are 22-mer oligonucleotides that are complementary to OBS

sites 1 and 2, respectively (**Fig. 6b**). Similarly, the allosteric dynamic range for OR-1 was estimated by examining the kinetics of ribozyme cleavage (**Fig. 6c**) in the absence of effector DNA (apparent $k_{obs} = 2.3 \times 10^{-4}$ min^{-1}) and in the presence of both DNA-9 and DNA-10 (apparent $k_{obs} = 0.9$ min^{-1}). The dynamic range of this ribozyme is ~4,000-fold under standard assay conditions. In an assay mixture that more closely approximates physiological conditions (50 mM Tris-HCl, pH 7.5 at 23 °C, 100 mM KCl, 25 mM NaCl, and 2 mM MgCl$_2$) the k_{obs} was found to be about 0.3 min^{-1} at 37 °C (data not shown). Similar to that observed with AND-1, the k_{obs} value for the OR-1 construct improved to 0.5 min^{-1} under these assay conditions when position 18 was mutated to a C residue (data not shown). Moreover, three additional constructs with OR logic function that respond to the same effector DNAs were created, which exhibited properties similar to those of OR-1 (**Supplementary Fig. 8** online).

Molecular circuit based on RNA switches with YES function

A possible attractive feature of molecular logic gates is the ability to generate signals that can control the activity of other molecular switches. The production of a diversity of oligonucleotide-sensing ribozymes would expand the complexity and efficiency of engineered nucleic acid circuits like those demonstrated previously[31,32].

To demonstrate inter-ribozyme communication, we used construct YES-1 and a variation of construct YES-2 to create a simple molecular circuit (**Fig. 7a**). The sequence and length of YES-2 was altered in stem I to create a YES-2 variant that generates a new 21-nt 3′ fragment upon self-cleavage (**Fig. 7a**). This RNA fragment is complementary to the OBS of YES-1, and therefore it should activate the second ribozyme upon cleavage and dissociation from the first ribozyme in the circuit.
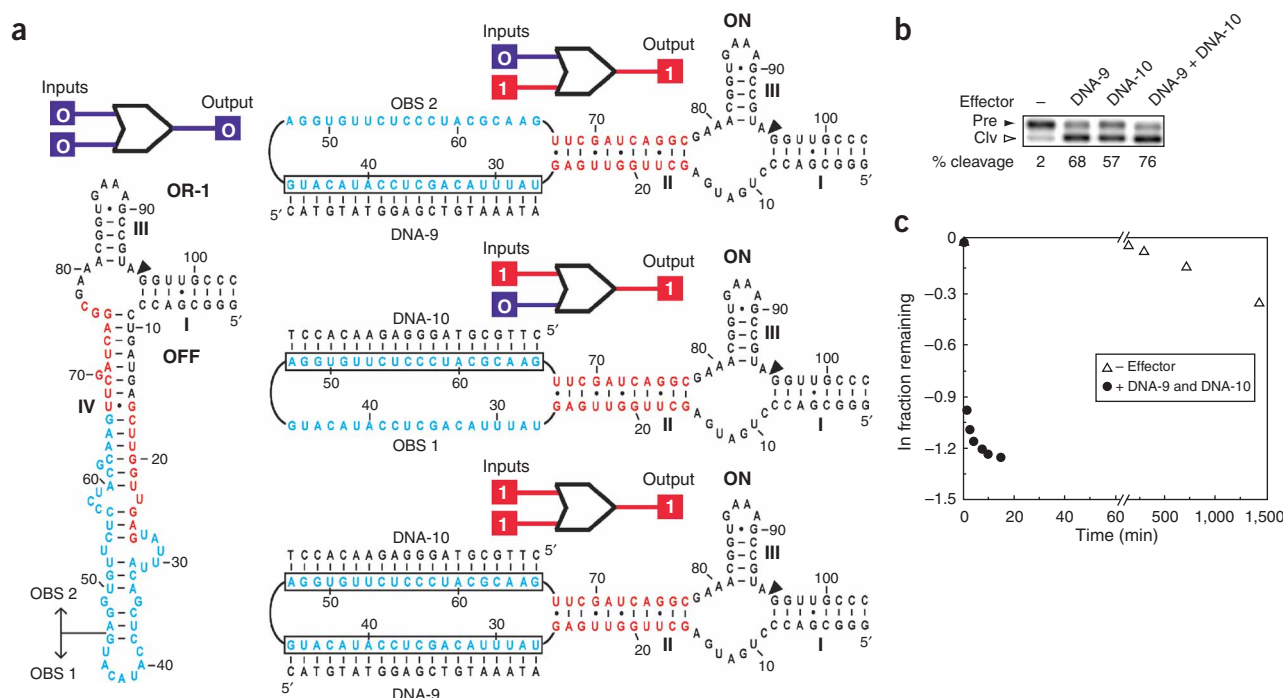
Figure 6 Design and characterization of OR-1, an oligonucleotide-specific molecular switch that possesses OR logic function. (**a**) OR-1 is designed to trigger self-cleavage when either effector (DNA-9 or DNA-10) or both effectors are present. Dot matrix plots for each of the four structures are presented in **Supplementary Figure 7** online. (**b**) Activation of OR-1 self-cleavage occurs when either or both effectors are present when incubated for 5 min under standard assay conditions. (**c**) Kinetics of OR-1 self-cleavage in the absence of effector and in the presence of both effector DNAs. Details are as described in the legend to **Figure 2**.
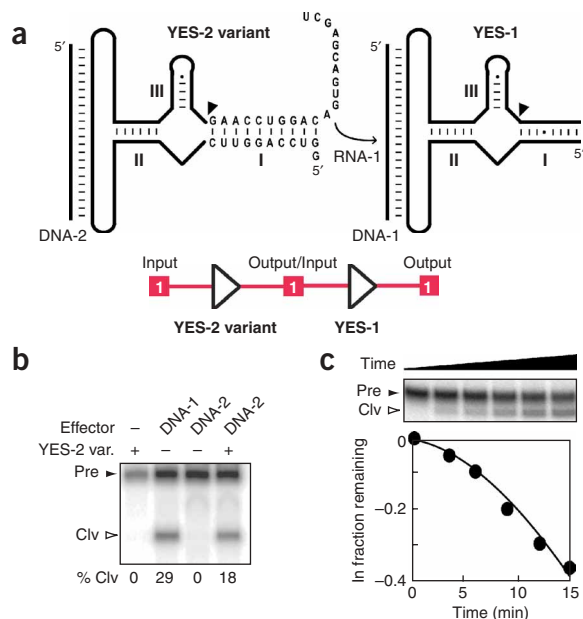
Figure 7 A two-step ribozyme signaling pathway constructed using YES-1 and a variant of YES-2. (**a**) Nucleotides of the YES-2 variant RNA that differ from YES-2 are depicted. Upon activation of YES-2 variant by effector DNA-2, the 3′ cleavage fragment (RNA-1) is released and serves as an effector for YES-1 activation. (**b**) Assay depicting function of a ribozyme-signaling pathway. YES-1 RNAs are radiolabeled in all lanes. Ribozymes and effector DNAs are present as defined at concentrations of 1 and 3 μM, respectively, and reactions were incubated at 23 °C for 5 min. Other details are as described for **Figure 2**. (**c**) Kinetic analysis of YES-1 self-cleavage in the presence of YES-2 variant and its effector DNA-2. Details are as described in **b**.

rate constants for cleavage once activated. This high probability of choosing functional designs is possible because the principles of RNA secondary-structure folding largely follow the simple rules of Watson-Crick base pairing, and the thermodynamic parameters for base-pair interactions are available.

One important advantage of the designs generated by this computational approach is that elements of the constructs can be treated as tunable modules, which makes possible the generation of large numbers of ribozymes with tailored functions by making only a few rational changes. This modularity can be exploited to more rapidly produce variant RNA switches that exhibit distinct effector specificities compared with *in vitro* selection, which might have to be repeated for each new target oligonucleotide. Even more sophisticated RNA switches that further mimic the properties of natural ribo-switches (e.g., cooperative ligand binding[57]) or that exhibit more complex sensory and control functions might be computationally engineered. However, precise control over the folding and function of the RNA constructs must be retained or the designs will result in progressive erosion of ribozyme activity as more features are added.

The application of a partition function algorithm for computing base-pairing probabilities[44] allows RNA engineers to estimate the likelihood that certain secondary structure elements will form preferentially over others, and the computing power of desktop systems permits one to survey the full RNA energy landscape for millions of possible sequences with a reasonable expenditure of time. With only a few days of computational time, the scale of the different effector and ribozyme sequences explored could match the initial pool size sometimes used for *in vitro* selection experiments ($\sim 10^{15}$ molecules). Running several computational processes simultaneously would further reduce the computational time needed for these analyses to only a few hours.

Although the design process used here accounts for the thermodynamic stability of various base-paired structures in the absence or presence of effector oligonucleotides, it does not autonomously examine all aspects that determine the compatibility of structures formed by effector binding and structures required for catalysis. For example, the linkers between the OBS and stem II of the ribozyme for both YES-1 (**Fig. 2a**) and YES-2 (**Fig. 3a**) appear to constrain the distance between the end of an OBS-effector helix and one end of stem II of the ribozyme. This distance-constraint problem becomes even more evident in the designs of NOT-1 and OR-1. For example, the OR-1 secondary structure model as depicted (**Fig. 6a**) would require a 180° turn of the RNA backbone to accommodate two rigidly formed OBS-effector interactions. Since this structure might be substantially strained, the RNAs might carry localized variations compared with the secondary structure models depicted. Whether all the base pairs involved in these two interactions can form simultaneously as modeled, or whether some base pairs must be denatured or otherwise distorted to approximate this secondary structure model is not considered by our current algorithm. Although these possible requirements for structural distortion do not prevent the computational design approach from providing functional RNA switches, future design efforts undoubtedly would be improved by taking into account these higher-ordered conformational features.

Most engineered ribozymes described in this study are based on a minimized version of the hammerhead ribozyme that typically exhibits a rate constant for RNA cleavage of no greater than 1 min^{−1}. Therefore, engineered oligonucleotide-responsive ribozymes based on this catalytic RNA are limited in their speed and possible

This simple molecular signaling pathway was demonstrated using radiolabeled YES-1 with various combinations of unlabeled YES-2 and the oligonucleotides DNA-1 and DNA-2. Although DNA-1 triggers YES-1 cleavage as demonstrated previously (**Fig. 2**), no cleavage is observed when both ribozymes are simultaneously incubated in the absence of DNA effector (**Fig. 7b**). This demonstrates that the YES-1 ribozyme is not activated when its RNA-1 signal oligonucleotide remains attached to the YES-2 variant ribozyme. In contrast, the addition of DNA-2 induces YES-1 cleavage only when the YES-2 variant ribozyme is present. Furthermore, the kinetics of YES-1 function as part of the complete signaling pathway are indicative of a lag phase that we interpret to be caused by the time required to release RNA-1 from the YES-2 variant upon activation by DNA-2 (**Fig. 7c**).

These findings are consistent with the design of a ribozyme-signaling pathway in which an activator of the first ribozyme in the series triggers release of an activator of the second ribozyme. Although this circuit is simple in design, our findings suggest that one could construct more complex molecular circuitries in which oligonucleotide triggers carry out various logic-based ribozyme functions.

DISCUSSION

In this study, we have used a computational approach to design various oligonucleotide-responsive ribozymes. Of 11 designs constructed based on the general architectures depicted in **Figure 1**, all of them functioned as robust RNA switches that exhibit at least three orders of magnitude in rate enhancement and large

utility. For example, the most active ribozymes designed in this study might not be sufficiently fast to influence the expression of genes in bacteria, which exhibit lifetimes that are typically measured in seconds or minutes. However, slightly larger variants of this ribozyme core[53–56] catalyze RNA cleavage with rate constants that are as large as 10^4 min^{-1}. Therefore, engineered constructs based on these enhanced self-cleaving ribozymes, such as NOT-1 (**Fig. 4**), could serve as high-speed oligonucleotide-responsive switches for building more complicated computational circuits[31,32] and biosensor devices[1]. High-speed RNA switches also could be used as components of designer genetic circuits[25,58–60]. Multiple different oligonucleotide-sensing ribozymes could be embedded within different reporter gene constructs with overall architectures that enable sensing the expression of mRNAs, noncoding nucleic acids or externally delivered oligonucleotide effectors.

METHODS

Design of RNA switches possessing different logic functions. The design of oligonucleotide-specific allosteric ribozymes was performed in two stages by adapting an existing random search algorithm for generating DNA libraries for molecular computing[61]. In stage 1, four different types of hammerhead ribozymes representing AND, OR, YES and NOT Boolean logic functions were selected by computing RNA secondary structures based on the equilibrium partition function as described by McCaskill[44]. Our use of this approach relies on the application of thermodynamic parameters using essentially the RNAfold source code from the Vienna RNA folding package[62–64].

For three switch types (AND, OR and YES), constructs were designed such that the nucleotides forming stem II of the hammerhead were held constant, whereas the adjoining loop sequences were randomized. The search algorithm selects for variations of loop sequences that permit portions of the stem II pairing elements to form alternative structure in the absence of effector DNAs. The design of the NOT construct was conducted using the same search algorithm, but the loop sequences adjoining stem III were varied. To simulate the presence of the effector DNA the nucleotides within the OBS elements are defined as having no potential to form secondary structure with the remainder of the construct. Two different states representing the absence and presence of DNA effector were computed for YES and NOT gates. Four different states were computed for OR and AND gates.

In stage 2, the different types of RNA switches were used as matrices for generating sets of ribozyme constructs that have OBS elements with distinct sequences. For example, the random search algorithm applied for the design of YES gates for stage 1 (1.X) and stage 2 (2.X) is outlined below. See also a flow chart for this computational procedure depicted in **Supplementary Figure 9** online.

1.1. Generate a new random OBS, from 16 to 22 nt long, over the alphabet of A, U, C, G. The sequences should not have four or more consecutive identical nucleotides.

1.2. Insert the OBS into the predefined RNA sequence GGGCGACCCU GAUGAGCUUGAGUUU(X)$_{16-22}$AUCAGGCGAAACGGUGAAAGCCGUAGG UUGCCC that contains the hammerhead motif.

1.3. Fold the sequence obtained and calculate the free energy at 37 °C of the structure using the partition function.

1.4. Determine whether nucleotides 3 through 9 of the hammerhead core (**Fig. 1a**) participate in base-pair formation in the dominant OFF state secondary structure using the probability dot matrix plot derived from the partition function. If one or more nucleotides 3 through 9 remain unpaired, reject the sequence and go to 1.1.

1.5. Replace the OBS from the structure with the same number of artificial nucleotides that are defined to have no binding properties.

1.6. Fold the sequence and compute the free energies of this ON state based on the partition function.

1.7. Determine if the resulting dominant structure carries all three stems that are required for function of the hammerhead ribozyme using the probability dot matrix plot derived from the partition function. If there is not such a dominant structure, reject the sequence and go to 1.1.

1.8. Determine the percentage of nucleotides in the OBS that participate in base-pairing interactions in the absence of DNA effector. If this value is <30% or >70%, reject the sequence and go to 1.1.

1.9. Compute the free energy of the dominant OFF state secondary structure based on the partition function and determine the gap between the OFF and ON state free energies. If the energy gap is outside the range –6 and –10 kcal mol^{-1}, reject the sequence and go to 1.1. This gap was chosen based on an estimate of the balance between maintaining a stable OFF state and rapidly overcoming this stability via the energy of DNA effector binding.

1.10: Run the program RNAheat (Vienna RNA folding package) for the ON and OFF states. If the dominant structures are not preserved in the range from 20 to 40 °C, reject sequence and go to 1.1.

1.11. Compute the ensemble diversity for OFF and ON states. If it does not exceed 9 units (higher values indicate greater secondary structure variability)[61], register the sequence as a candidate and go to 1.1. Registered candidates are further processed on an individual basis starting with 2.1.

2.1. Using the secondary structure generated by the stage 1 algorithm wherein the OBS is excluded (see below; parentheses identify base-paired nucleotides), calculate the thermodynamic stability of the structure. Run the program RNAinverse (Vienna RNA folding package) program to generate new RNA sequence that possesses similar secondary structure folding but random sequence of the OBS.

```
((((((((((((((((((((((.(..(((......))).
gggcgacccugaugagcuugaguuuXXXXXXXXXXX
))))))))))))))).....(((((....)))))).)))))))))
XXXXXXXXXXaucaggcgaaacggugaaagccguagguugccc
```

2.2. Determine whether nucleotides 3 through 9 of the hammerhead core (**Fig. 1a**) participate in base-pair formation of the dominant secondary structure using the probability matrix derived from the partition function. If one or more nucleotides 3 through 9 remain unpaired, reject the RNA sequence and go to 2.1.

2.3. Compute the thermodynamic stability of the dominant secondary structure provided in step 2.2. If the thermodynamic stability of the structure differs by more than ± 5% compared to the candidate RNA sequence provided in step 1.11, reject the sequence and go to 2.1.

2.4. Compute the thermodynamic stability of the OBS bound to its perfectly matched complement RNA. If the thermodynamic stability of the duplex differs by more than ± 5% compared to the candidate OBS provided in step 1.11, reject the sequence and go to 2.1.

2.5. Run the program RNAheat[61] for the ON and OFF states. If the dominant structures are not preserved in the range from 20 to 40 °C, reject sequence and go to 2.1. The selection of constructs that satisfy this criterion help assure that the RNA switches will function at 23 °C, despite thermodynamic modeling with data established at 37 °C.

2.6. Run the program kinRNA[49] with the RNA sequence derived from stem 2.5. If the dominant structure is not folded within 480 units (larger arbitrary units indicate slower folding), reject sequence and go to 2.1.

2.7. Compute the free energy of the dominant OFF state secondary structure based on the partition function and determine the gap between the OFF and ON state free energies. If the energy gap is more than twofold different than the candidate sequence derived in step 1.11, reject the sequence and go to 2.1.

The procedure applied for the selection of AND, OR and NOT gates utilizes a similar progression of steps. For the AND and OR gates, additional steps were added to compute the structural properties when either one or both effectors are present.

Oligonucleotides. Synthetic DNAs were obtained from Keck Biotechnology Resource Laboratory (Yale University). DNAs were purified by denaturing (8 M urea) PAGE before use. Template DNAs for *in vitro* transcription were prepared by overlap extension using SuperScript II reserve transcriptase (Invitrogen) in a reaction volume of 50 μl according to the manufacturer's instructions. Synthetic DNAs corresponding to the nontemplate strand each carried a T7 RNA promoter sequence (TAATACGACTCACTATA) and 15 nucleotides at the 3′ terminus that overlapped with the synthetic DNA corresponding to the template strand. The resulting double-stranded DNAs were recovered by

precipitation with ethanol and used as templates for transcription *in vitro* (RiboMax; Promega) in the presence of α-^{32}P ATP according to the manufacturer's directions. The transcribed RNAs, produced during a 2-h incubation, were isolated by using denaturing 10% PAGE.

Allosteric ribozyme assays. Radiolabeled RNAs were incubated at 25 °C in a reaction solution containing 100 mM Tris-HCl, (pH 8.3 at 23 °C) and 10 mM MgCl$_2$. NOT-1 ribozyme assays were conducted at 37 °C in a solution containing 2 mM MgCl$_2$, 100 mM KCl, 25 mM NaCl, 50 mM Tris-HCl (pH 7.5 at 37 °C). Ribozyme reactions were initiated by the addition of MgCl$_2$ after pre-incubating NOT-1 and tenfold excess DNA-6 (when present) for 5 min in Mg^{2+}-free reaction buffer. Reactions were terminated by the addition of an equal volume of gel loading buffer containing 200 mM EDTA. The reaction products were analyzed using denaturing 10% or 6% PAGE and the product bands were detected and quantified using a PhosphorImager (Molecular Dynamics). Rate constants were determined by plotting the natural logarithm of the fraction of RNA remaining uncleaved versus time, wherein the negative slope of the resulting line reflects k_{obs}.

Note: Supplementary information is available on the Nature Biotechnology website.

COMPETING INTERESTS STATEMENT
The authors declare competing financial interests (see the *Nature Biotechnology* website for details).

1. Breaker, R.R. Natural and engineered oligonucleotides as tools to explore biology. *Nature* **432**, 838–845 (2004).
2. Gold, L., Polisky, B., Uhlenbeck, O.C. & Yarus, M. Diversity of oligonucleotides functions. *Annu. Rev. Biochem.* **64**, 763–797 (1995).
3. Osborne, S.E. & Ellington, A.D. Nucleic acid selection and the challenge of combinatorial chemistry. *Chem. Rev.* **97**, 349–370 (1997).
4. Hamaguchi, N., Ellington, A. & Stanton, M. Aptamer beacons for the detection of proteins. *Anal. Biochem.* **294**, 126–131 (2001).
5. McCauley, T.G., Hamaguchi, N. & Stanton, M. Aptamer-based biosensor arrays for detection and quantification of biological macromolecules. *Anal. Biochem.* **319**, 244–250 (2003).
6. Bock, C. *et al.* Photoaptamer arrays applied to multiplexed proteomic analysis. *Proteomics* **4**, 609–618 (2004).
7. Soukup, G.A. & Breaker, R.R. Nucleic acid molecular switches. *Trends Biotechnol.* **17**, 469–476 (1999).
8. Soukup, G.A. & Breaker, R.R. Allosteric nucleic acid catalysts. *Curr. Opin. Struct. Biol.* **10**, 318–325 (2000).
9. Silverman, S.K. Rube Goldberg goes (ribo)nuclear? Molecular switches and sensors made from RNA. *RNA* **9**, 377–383 (2003).
10. Seetharaman, S., Zivarts, M., Sudarsan, N. & Breaker, R.R. Immobilized RNA switches for the analysis of complex chemical and biological mixtures. *Nat. Biotechnol.* **19**, 336–341 (2001).
11. Hesselberth, J.R., Robertson, M.P., Knudsen, S.M. & Ellington, A.D. Simultaneous detection of diverse analytes with an aptazyme ligase array. *Anal. Biochem.* **312**, 106–112 (2003).
12. Nahvi, A. *et al.* Genetic control by a metabolite binding mRNA. *Chem. Biol.* **9**, 1043–1049 (2002).
13. Winkler, W., Nahvi, A. & Breaker, R.R. Thiamine derivatives bind messenger RNAs directly to regulate bacterial gene expression. *Nature* **419**, 952–956 (2002).
14. Mironov, A.S. *et al.* Sensing small molecules by nascent RNA: a mechanism to control transcription in bacteria. *Cell* **111**, 747–756 (2002).
15. Winkler, W.C., Cohen-Chalamish, S. & Breaker, R.R. An mRNA structure that controls gene expression by binding FMN. *Proc. Natl. Acad. Sci. USA* **99**, 15908–15913 (2002).
16. Sudarsan, N., Barrick, J.E. & Breaker, R.R. Metabolite-binding RNA domains are present in the genes of eukaryotes. *RNA* **9**, 644–647 (2003).
17. Kubodera, T. *et al.* Thiamine-regulated gene expression of *Aspergillus oryzae thiA* requires splicing of the intron containing a riboswitch-like domain in the 5′ UTR. *FEBS Lett.* **555**, 516–520 (2003).
18. Winkler, W.C. & Breaker, R.R. Genetic control by metabolite-binding riboswitches. *ChemBioChem* **4**, 1024–1032 (2003).
19. Vitreschak, A.G., Rodionov, D.A., Mironov, A.A. & Gelfand, M.S. Riboswitches: the oldest mechanism for the regulation of gene expression. *Trends Genet.* **20**, 44–50 (2004).
20. Mandal, M. & Breaker, R.R. Gene regulation by riboswitches. *Nat. Rev. Mol. Cell Biol.* **5**, 451–463 (2004).
21. Lewin, A.S. & Hauswirth, W.W. Ribozyme gene therapy: applications for molecular medicine. *Trends Mol. Med.* **7**, 221–228 (2001).
22. Schubert, S. & Kurreck, J. Ribozyme- and deoxyribozymes-strategies for medical applications. *Curr. Drug Targets* **5**, 667–681 (2004).
23. Werstuck, G. & Green, M.R. Controlling gene expression in living cells through small molecule-RNA interactions. *Science* **282**, 296–298 (1998).
24. Grate, D. & Wilson, C. Inducible regulation of the *S. cerevisiae* cell cycle mediated by an RNA aptamer-ligand complex. *Bioorg. Med. Chem.* **9**, 2565–2570 (2001).
25. Thompson, K.M., Syrett, H.A., Knudsen, S.M. & Ellington, A.D. Group I aptazymes as genetic regulatory switches. *BCM Biotechnol.* **2**, 21 (2002).
26. Suess, B., Fink, B., Berens, C., Stenz, R. & Hillen, W. A theophylline responsive riboswitch based on helix slipping controls gene expression *in vivo*. *Nucleic Acids Res.* **32**, 1610–1614 (2004).
27. Desai, S.K. & Gallivan, J.P. Genetic screens and selections for small molecules based on a synthetic riboswitch that activates protein translation. *J. Am. Chem. Soc.* **126**, 13247–13254 (2004).
28. Breaker, R.R. Engineered allosteric ribozymes as biosensor components. *Curr. Opin. Biotechnol.* **13**, 31–39 (2002).
29. Ferguson, A. *et al.* A novel strategy for selection of allosteric ribozymes yields RiboReporter sensors for caffeine and aspartame. *Nucleic Acids Res.* **32**, 1756–1766 (2004).
30. Srinivasan, J. *et al.* ADP-specific sensors enable universal assay of protein kinase activity. *Chem. Biol.* **11**, 499–508 (2004).
31. Stojanovic, M.N. & Stefanovic, D. Deoxyribozyme-based half-adder. *J. Am. Chem. Soc.* **125**, 6673–6676 (2003).
32. Stojanovic, M. & Stafanovic, D. A deoxyribozyme-based molecular automaton. *Nat. Biotechnol.* **21**, 1069–1074 (2003).
33. Tang, J. & Breaker, R.R. Rational design of allosteric ribozymes. *Chem. Biol.* **4**, 453–459 (1997).
34. Jose, A.M., Soukup, G.A. & Breaker, R.R. Cooperative binding of effectors by an allosteric ribozyme. *Nucleic Acids Res.* **29**, 1631–1637 (2001).
35. Soukup, G.A. & Breaker, R.R. Engineering precision RNA molecular switches. *Proc. Natl. Acad. Sci. USA* **96**, 3584–3589 (1999).
36. Koizumi, M., Kerr, J.K., Soukup, G.A. & Breaker, R.R. Allosteric ribozymes sensitive to the second messengers cAMP and cGMP. *Nat. Struct. Biol.* **6**, 1062–1071 (1999).
37. Robertson, M.P., Knudsen, S.M. & Ellington, A.D. *In vitro* selection of ribozymes dependent on peptides for activity. *RNA* **10**, 114–127 (2004).
38. Porta, H. & Lizardi, P.M. An allosteric hammerhead ribozyme. *Biotechnol.* **13**, 161–164 (1995).
39. Komatsu, Y., Yamashita, S., Kazama, N., Nobuoka, K. & Ohtsuka, E. Constructuion of new ribozymes requiring short regulator oligonucleotides as a cofactor. *J. Mol. Biol.* **299**, 1231–1243 (2000).
40. Burke, D.H., Ozerova, N.D. & Nilsen-Hamilton, M. Allosteric hammerhead ribozyme TRAPs. *Biochemistry* **41**, 6588–6594 (2002).
41. Wickiser, J.K., Cohen-Chalamish, S., Puskarz, I., Sawiki, B., Ward, D.C. & Breaker, R.R. Engineered oligonucleotides-responsive ribozymes that form structures resembling kissing complexes. (in preparation).
42. Stojanovic, M.N., Mitchell, T.E. & Stefanovic, D. Deoxyribozyme-based logic gates. *J. Am. Chem. Soc.* **124**, 3555–3561 (2002).
43. Wang, D.Y., Lai, B.H., Feldman, A.R. & Sen, D. A general approach for the use of oligonucleotides effectors to regulate the catalysis of RNA-cleaving ribozymes and DNAzymes. *Nucleic Acids Res.* **30**, 1735–1742 (2002).
44. McCaskill, J.S. The equilibrium partition function and base pair binding probabilities for RNA secondary structure. *Biopolymers* **29**, 1109–1119 (1990).
45. Bonhoeffer, S., McCaskill, J.S., Stadler, P.F. & Schuster, P. RNA multi-structure landscapes. A study based on temperature dependent partition functions. *Eur. Biophys. J.* **22**, 13–24 (1993).
46. Russell, R. *et al.* Exploring the folding landscape of a structured RNA. *Proc. Natl. Acad. Sci. USA* **99**, 155–160 (2002).
47. Woodson, S.A. Folding mechanisms of group I ribozymes: Role of stability and contact order. *Biochem. Soc. Trans.* **30**, 1166–1169 (2002).
48. Sosnick, T.R. & Pan, T. RNA folding: Models and perspectives. *Curr. Opin. Struct. Biol.* **13**, 309–316 (2003).
49. Flamm, C., Fontana, W., Hofacker, I. & Schuster, P. RNA folding kinetics at elementary step resolution. *RNA* **6**, 325–338 (2000).
50. Flamm, C., Hofacker, I.L., Maurer-Stroh, Stadler, P.F. & Zehl, M.S. Design of multi-stable RNA molecules. *RNA* **7**, 254–265 (2001).
51. Forster, A.C. & Symons, R.H. Self-cleavage of plus and minus RNAs of a virusoid and a structural model for the active sites. *Cell* **49**, 211–220.
52. Hertel, K.J. *et al.* Numbering system for the hammerhead. *Nucleic Acids Res.* **20**, 3252 (1992).
53. Osborne, E.M., Schaak, J.E. & DeRose, V.J. Characterization of a native hammerhead ribozyme derived from schistosomes. *RNA* **11**, 187–196 (2005).
54. Khvorova, A., Lescoute, A., Westhof, E. & Jayasena, S.D. Sequence elements outside the hammerhead ribozyme catalytic core enable intracellular activity. *Nat. Struct. Biol.* **10**, 708–712 (2003).

55. De la Pena, M., Gago, S. & Flores, R. Peripheral regions of natural hammerhead ribozymes greatly increase their self-cleavage activity. *EMBO J.* **22**, 5561–5570 (2003).

56. Canny, M.D. *et al.* Fast cleavage kinetics of a natural hammerhead ribozyme. *J. Am. Chem. Soc.* **126**, 10848–10849 (2004).

57. Mandal, M. *et al.* A glycine-dependent riboswitch that uses cooperative binding to control gene expression. *Science* **306**, 275–279 (2004).

58. Yen, L. *et al.* Exogenous control of mammalian gene expression through modulation of RNA self-cleavage. *Nature* **431**, 471–476 (2004).

59. Bayer, T.S. & Smolke, C.D. Programmable ligand-controlled riboregulators of eukaryotic gene expression. *Nat. Biotechnol.* **23**, 337–343 (2005).

60. Isaacs, F.J. *et al.* Engineered riboregulators enable post-transcriptional control of gene expression. *Nat. Biotechnol.* **22**, 841–847 (2004).

61. Penchovsky, R. & Ackermann, J. DNA library design for molecular computation. *J. Comput. Biol.* **10**, 215–229 (2003).

62. Mathews, D., Sabina, J., Zucker, M. & Turner, H. Expanded sequence dependence of thermodynamic parameters provides robust prediction of RNA secondary structure. *J. Mol. Biol.* **288**, 911–940 (1999).

63. Hofacker, I.L. *et al.* Fast folding and comparison of RNA secondary structures. *Monatsh. Chem.* **125**, 167–188 (1994).

64. Hofacker, I.L. Vienna RNA secondary structure server. *Nucleic Acids Res.* **31**, 3429–3431 (2003).